ASTRONOMY & ASTROPHYSICS
SUPPLEMENT SERIES

Astron. Astrophys. Suppl. Ser. **118,** 397-405 (1996)

Irregular variables of type Lb. New $JHKL'M$-photometry for 160 stars⋆

F. Kerschbaum[1], C. Lazaro[2,3] and P. Habison[1]

[1] Institut für Astronomie der Universität Wien, Türkenschanzstraße 17, A-1180 Wien, Austria
[2] Dpto. de Astrofísica, Fac. de Física, Universidad de La Laguna, 38200-La Laguna, Tenerife, Spain
[3] Instituto de Astrofísica de Canarias, 38200-La Laguna, Tenerife, Spain

Received August 16; accepted January 10, 1996

Abstract. — This paper presents new near infrared observations of 160 Irregular variables of type Lb in the $JHKL'M$ filter bands. These measurements are supplemented by data for additional 56 stars taken from the literature. In total 220 datasets are available because of some multiple observations. From our sample, 216 stars have near infrared (NIR) photometry now. Our sample of visually bright Lb-variables displays very similar infrared properties when compared with SRa- and SRb-variables. Derived from NIR-two colour diagrams the oxygen-rich Lbs seem to have intermediate atmospheric conditions between Miras and normal giants. There may be a sligthly larger "contamination" with non AGB-giants than in the case of the semiregulars. Using only our IR-colours the S- and the Carbon-stars among the Lbs again are undistinguishable from SR-variables of the same chemistry.

Key words: stars: asymptotic giant branch (AGB) — stars: variables — stars: mass-loss — infrared: stars

1. Introduction

For a long time Mira variables, OH/IR- and Carbon-stars were the most frequently studied Asymptotic Giant Branch (AGB) objects. The Semiregular (types SRa and SRb) and the cool Irregular variables (Lb) – quite numerous groups of objects – have been almost neglected although their role within the evolution on the AGB and their overall properties are far from being understood. The can provide important constraints for theoretical models due to their different pulsational behaviour compared to the more frequently studied Mira variables.

Fortunately, this situation has changed during the last years – at least in the case of the Semiregulars. In Kerschbaum & Hron (1992, 1994, 1996, SR-Papers I, II, III respectively) and Kerschbaum (1995, SR-Paper IIb) stellar properties of Semiregular variables (SRVs) derived from GCVS4 (Kholopov et al. 1985–88), IRAS-PSC (1988) and IRAS-LRS (1986) as well as new near infrared photometry were used to divide this inhomogeneous group of objects into physically distinct classes and to probe their evolutionary status. A study by Jura & Kleinmann (1992) came to similar conclusions concerning the galactic distribution of these stars.

Complementing our work on SRVs, cool Irregular variables should be analysed in an analogous way. From what is known about the luminosities of Irregular variables of type Lb and since this group contains also Carbon stars, a significant number of Lbs should be on the thermally-pulsing AGB (see the review by Querci 1986). However, Little et al. (1987) found no Technetium in the O-rich Lbs of their sample whose presence would be an evidence for a recent thermal pulse.

Peters (1991) used data from the IRAS-mission for an analysis of the space distribution and the mass loss of the main three AGB-variables the Miras, the Semiregulars and the Irregulars. The main outcome concerning the latter is that Irregulars seem to have mass loss rates comparable to those of Semiregulars but smaller than those of Miras. He arrived at similar scale heights for all three groups except for the long period Miras which turned out to be more concentrated to the disk.

In a study mainly devoted to Semiregulars, Jura & Kleinmann (1992) derived a galactic distribution of the Irregular variables comparable to that of "thin disk" Miras. Unfortunately, their sample was a mixture of Irregulars with a significant number of Semiregulars and Miras with unknown periods. Moreover, it was limited to objects with $|b| \geq 30°$ having GCVS and IRAS-data. All these restrictions did not allow a more detailed analysis. Nevertheless,

Send offprint requests to: kerschbaum@astro.ast.univie.ac.at
⋆Based on observations collected at the European Southern Observatory, La Silla, Chile and on observations made with the Carlos Sánchez Telescope operated on the island of Tenerife by the Instituto de Astrofísica de Canarias (IAC) in the Observatorio del Teide, Izaña

these examples of recent publications in that field demonstrate the need for more work.

Since our approach needs data from the visual to the far infrared the first step was to close the gap in the stars energy distributions between the visual GCVS4 data and the $12-100\,\mu$m infrared range of the IRAS-PSC. We obtained new $JHKL'M$-photometry and supplemented it by 'photometrically compatible' data from the literature for a representative subsample of the Lb variables in the GCVS4. In order to derive bolometric magnitudes for volume limited samples of Lbs (compare SR-Paper I) – which we plan for a forthcoming paper – the objects presented in the paper will also act as prototypes providing us with the bolometric corrections needed for the stars lacking NIR-data.

2. Observations

A sample of optically bright GCVS4 variables of type Lb was selected by means of the availability of good photometry in the IRAS-PSC. Down to mean visual magnitudes of about $11\overset{\mathrm{m}}{.}5$ (typically $3\overset{\mathrm{m}}{.}5$ in filter K) nearly all stars accessible from the Canary Islands were observed. For the southern hemisphere no comparable systematic approach was tried – mainly literature data was used. Consequently, there is no well defined completeness level at any magnitude. When going to fainter magnitudes down to $13\overset{\mathrm{m}}{.}0$ in V the northern photometric completeness goes down to about 50%. Finally, for both hemispheres, only 9% of the observed stars or the listed literature objects is even fainter than $13\overset{\mathrm{m}}{.}0$ in V.

All sources were searched for at their GCVS4 positions, mostly in filter K. A diaphragm of $15''$ was used; beam-switching was done in the East-West direction with a throw of generally $20''$. Standard and programme stars were observed at similar air mass ranges to avoid the non-linear effects of atmospheric extinction in the infrared. The $JHKL'M$-photometry was calibrated on the Koornneef (1983a,b) system.

For the photometry at the European Southern Observatory the 1 m telescope equipped with its standard infrared photometer was used. It has to be noted that the ESO L-filter is actually L' ($3.78\,\mu$m instead of $3.6\,\mu$m for the original Johnson L) but the ESO standards are in L and taken from Koorneef (1983a). The consequences are discussed in Kerschbaum & Hron (1994). The observations were done by FK in collaboration with C. Loup in 1994 in the course of another observing programme. Additional old observations were kindly provided by F. Guglielmo. All the new ESO-datasets are labeled with 'M' in Table 3 whereas the old data are labeled with 'K'.

At the Observatorio del Teide the 1.5 m "Carlos Sánchez Telescope" of the Instituto de Astrofísica de Canarias (IAC) on Izaña, Tenerife was used with the "CVF Photometer-Spectrophotometer". Again the L-filter is actually L' ($3.78\,\mu$m). The observations were done by the authors during three dedicated runs in 1994 and 1995 and an additional one (November '94) again in collaboration with C. Loup. These datasets are labeled 'I' in Table 3.

3. Oxygen-rich Lb-variables

No reddening correction was applied to the new near infrared photometry. Interstellar reddening should not strongly influence the results of our rather local samples (when assuming luminosities of typically 5000 solar luminosities; compare SR-Paper I). Nevertheless, all of our figures containing infrared colours show "1 kpc"-reddening vectors using the absorption coefficients $A_J/A_V = 0.246$, $A_H/A_V = 0.141$, $A_K/A_V = 0.088$ and $A_L/A_V = 0.046$ taken from Feast et al. (1982). $A_{12\,\mu\mathrm{m}}/A_V = 0.048$ and $A_{25\,\mu\mathrm{m}}/A_V = 0.005$ come from Wainscoat et al. (1992).

In order to compare groups of defined chemistry the stars were classified according to both their optical spectral classes taken from the GCVS4 and mid-infrared spectral types taken from the IRAS-LRS. For details see SR-Paper I.

Since for a given chemistry the colours are mainly temperature dependent, each chemistry group has to be discussed separately.

To facilitate the comparison with O-rich SRVs, the typical colour-ranges of their two main groups, namely the 'blue' and the 'red' ones are plotted together with the new measurements of the O-rich Lbs in Fig. 1. As shown in SR-Paper I, we think that the blue SRVs are on the early AGB, whereas the red SRVs seem to be on the thermally pulsing AGB. Moreover the locus of Me-Miras (Feast et al. 1982) and that of non variable M giants in the solar neighbourhood are indicated (Feast et al. 1990) in the plot. The colours of Me-Miras and M giants were transformed from the SAAO to the ESO photometric system using the results of SR-Paper II.

Differences in effective temperature and possibly atmospheric extension, influencing the strength of the H_2O absorption band and the continuum shape in the photometric H band, are responsible for the separation in that particular two colour diagram (Bessell et al. 1989).

Only a negligible fraction of the O-rich Lbs are located in the Mira domain; the large majority shows a similar distribution as the O-rich SRVs lying between the Me-Miras and the M-giant line. A few objects extend the distribution towards bluer J–H colours along the M-giant line. These stars may be not on the AGB at all. Using only near infrared colours the O-rich Lbs are undistinguishable from SRVs with the same chemistry.

4. Identification of Carbon stars

Near-infrared together with IRAS photometry can be used to separate O-rich from C-rich stars (see Epchtein et al. 1987; Epchtein et al. 1990; Guglielmo et al. 1993).

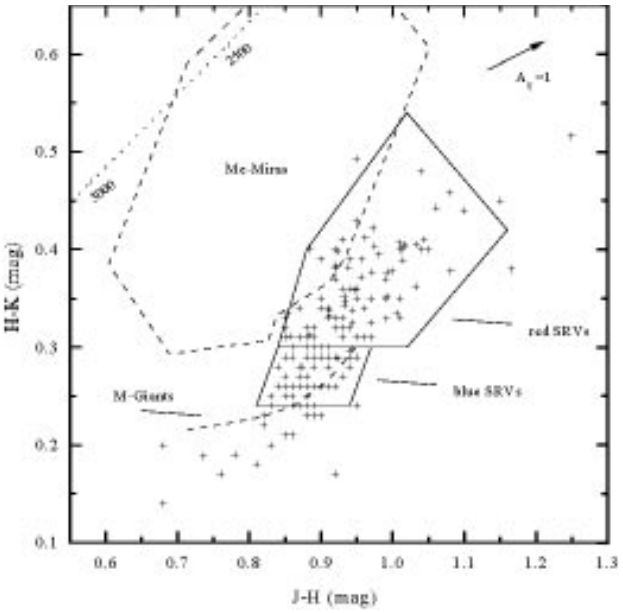

Fig. 1. Near infrared two colour diagram of O-rich Lb variables. The regions where blue and red SRVs are found are indicated by full lines. The dashed box is the area occupied by Me-Miras taken from Feast et al. (1982). The bowed, dashed line is the mean locus of non-variable M giants in the solar neighbourhood (Feast et al. 1990). The colours of Me-Miras and M-Giants were transformed from the SAAO to the ESO photometric system using the results of Kerschbaum & Hron (1994). The colours for blackbodies of different temperatures [K] are indicated. A reddening vector displays the colour shift for $A_V = 1$

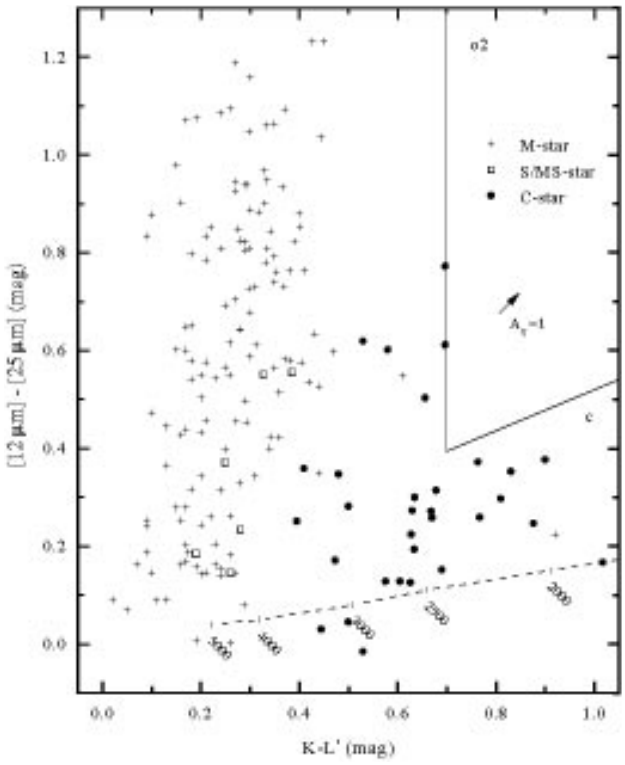

Fig. 2. Infrared two colour diagram of Lb variables according to that used by Epchtein et al. (1987) to discriminate O-rich against Carbon stars. Three different symbols denote O-rich, C-rich or S-stars, respectively. The colours for blackbodies of different temperatures [K] are indicated. A reddening vector displays the colour shift for $A_V = 1$

In Fig. 2 all Lbs having NIR-photometry and a 'chemical' classification originating from their visual- and IRAS-spectra are plotted in a K–L' versus [12]–[25] two colour diagram.

Some areas following Epchtein et al. (1987) are indicated – for K–$L' < 0.7$ and at low values of $[12\,\mu\mathrm{m}] - [25\,\mu\mathrm{m}]$ mostly dustless objects are found. At higher $[12\,\mu\mathrm{m}] - [25\,\mu\mathrm{m}]$, region o2 contains O-rich stars with increasing mass loss and finally in region c the probability of finding C-rich objects is very high.

As expected for our optically bright sample of AGB-stars, only a very small number of objects is found at high K–L' values. Most of the stars, especially the O-rich ones, are found in the regions of bare photospheres or thin circumstellar envelopes at K–$L' < 0.7$. In addition the Carbon stars populate the 'hot' parts of region c closer to the blackbody line than the O-rich objects.

The O-rich Lbs distribution extends from the *Rayleigh-Jeans point* where one finds the 'blue' SRVs of the SR-Papers I and II towards higher $[12\,\mu\mathrm{m}] - [25\,\mu\mathrm{m}]$ to the area of the 'red' SRVs. Maybe the gap between the two groups is less pronounced than it is the case for SRVs. C-rich Lbs display a significantly wider spread towards red K–L', similar to the distribution of SRs of the same chemistry.

5. Conclusion and outlook

From our sample 216 stars have near infrared (NIR) photometry, now. In total 220 datasets are available because of a few multiple observations.

The first analysis of the NIR-data presented in this paper can be summarized as follows: Our sample of visually bright Lb-variables displays very similar properties when compared with the SRa- and SRb-variables. Derived from NIR-two colour diagrams the oxygen-rich Lbs seem to have intermediate atmospheric conditions between Miras and normal giants. There may be a sligthly larger "contamination" with non AGB-giants than in the case of SRs. The S- and the Carbon-stars among the Lbs again are undistinguishable from SR-variables of the same chemistry.

In a forthcoming paper we will use the photometry presented in this paper to construct complete energy distributions from the visual, through the near to the far infrared. The parameters derived from blackbody fits through these

energy distributions will be discussed in terms of the pulsational properties of the Lbs (compare with SR-Paper III). Moreover, it will be tried to probe their galactic distribution and their evolutionary status, especially in relation to Semiregulars and Miras which were investigated in SR-Paper I. Finally, to complement the dust-mass-loss information derived from IRAS photometry by gas-mass-loss rates a CO-study comparable to that of Kerschbaum et al. (1996, SR-Paper IV) is forseen.

The evolution on the Asymptotic Giant Branch probably can only be understood by comparing all of the groups showing different pulsational behaviour. Irregulars, Semiregulars and Miras, all of them including objects at different evolutionary stages have to be taken into account to get an overall picture of the Asymptotic Giant Branch.

Acknowledgements. The authors would like to thank the referee T. Le Bertre for his constructive comments. J. Hron is acknowledged for his cooperative support. FK is grateful to C. Loup for fruitful collaboration. This work was supported by the *Fonds zur Förderung der wissenschaftlichen Forschung* under project numbers P9638-AST and S7308-AST. PH received a travel grant from the *Österreichische Forschungsgemeinschaft*. This research has made use of the Simbad database.

A. Appendix

Table 3 lists all near-infrared photometry (220 data sets for 216 stars) presented in this paper. Besides GCVS4- and IRAS-name, the Julian day number and a code 'c' denoting the origin of the data is given. 'c' is defined in Table 1 where the number of stars observed is also listed. In the case of literature data (code K) no Julian day number is available.

Table 1. Code of the observation

c	Observatory	Reference	data sets
I	IAC	new	138
M	ESO	new	24
K	ESO	Fouqué et al. (1992), Guglielmo et al. (1993)	58

Estimates of the mean total errors of the NIR-photometry taken at the two observatories are given in Table 2. For data originating from our own runs (M, I) the given values are calculated from the individual programme- and standard-star-measurements. The errors do not include uncertainties of the photometric system. For data sets with code K the accuracies are comparable to those with code M.

Table 2. Mean total errors of NIR-photometry

c	Mag.	σ_J	σ_H	σ_K	$\sigma_{L'}$	σ_M
M, K	< 3	$0\overset{m}{.}03$	$0\overset{m}{.}02$	$0\overset{m}{.}02$	$0\overset{m}{.}02$	$0\overset{m}{.}06$
	4	·	·	·	·	$0\overset{m}{.}08$
	5	·	·	·	$0\overset{m}{.}03$	$0\overset{m}{.}15$
	6	$0\overset{m}{.}05$	$0\overset{m}{.}05$	$0\overset{m}{.}05$	$0\overset{m}{.}05$	$0\overset{m}{.}20$
	7−8	$0\overset{m}{.}06$				$0\overset{m}{.}40$
I	< 3	$0\overset{m}{.}03$	$0\overset{m}{.}03$	$0\overset{m}{.}03$	$0\overset{m}{.}03$	
	4	·	·	·	·	
	5	·	·	·	$0\overset{m}{.}05$	
	6	$0\overset{m}{.}04$	$0\overset{m}{.}04$	$0\overset{m}{.}04$	$0\overset{m}{.}06$	
	7−9	$0\overset{m}{.}06$	$0\overset{m}{.}06$	$0\overset{m}{.}06$		

References

Bessell M.S., Brett J.M., Scholz M., Wood P.R., 1989, A&A 213, 209
Epchtein N., Le Bertre T., Lepine J.R.D., et al., 1987, A&AS 71, 39
Epchtein N., Le Bertre T., Lepine J.R.D., 1990, A&A 227, 82
Feast M.W., Robertson B.S.C., Catchpole R.M., et al., 1982, MNRAS 201, 439
Feast M.W., Whitelock P.A., Carter B.S., 1990, MNRAS 247, 227
Fouqué P., Le Bertre T., Epchtein N., Guglielmo F., Kerschbaum F., 1992, A&AS 93, 151
Guglielmo F., Epchtein N., Le Bertre T., et al., 1993, A&AS 99, 31
IRAS Science Team, 1986, A&AS 65, 607 (IRAS-LRS)
IRAS Science Team, 1988, IRAS Catalogs and Atlases, Vols. 2–6, NASA RP–1190 (IRAS-PSC)
Jura M., Kleinmann S.G., 1992, ApJS 79, 105
Kerschbaum F., 1995, A&AS 113, 441 (SR-Paper IIb)
Kerschbaum F., Hron J., 1992, A&A 263, 97 (SR-Paper I)
Kerschbaum F., Hron J., 1994, A&AS 106, 397 (SR-Paper II)
Kerschbaum F., Hron J., 1996, A&A 308, 489 (SR-Paper III)
Kerschbaum F., Olofsson H., Hron J., 1996, A&A, (in press) (SR-Paper IV)
Kholopov P.N., et al., 1985–88, General Catalogue of Variable Stars, 4th edition, "Nauka" Publishing House, Moscow (GCVS4)
Koornneef J., 1983a, A&AS 51, 489
Koornneef J., 1983b, A&A 128, 84
Little S.J., Little-Marenin I.R., Hagen Bauer W., 1987, AJ 94, 981
Peters W.J., 1991, Master Thesis, Univ. Amsterdam.
Querci F.R., 1986, The M-type stars. In: H.R. Johnson, F.R. Querci (eds.), NASA SP–492, p. 1–113
Wainscoat R.J., Cohen M., Volk K., Walker H.J., Schwartz D.E., 1992, ApJS 83, 111

Table 3. Near-infrared photometry

GCVS4	IRAS	JD	J	H	K	L'	M	c
And AU	01443+3932	2449587.070	5.23	4.32	4.02	3.74		I
And BC	22586+4614	2449669.869	2.35	1.44	1.11	1.02		I
And BZ	00348+4519	2449587.103	3.14	2.25	1.97	1.86		I
And CE	01265+4624	2449587.162	3.52	2.53	2.18	2.01		I
And CF	23013+3735	2449591.096	2.24	1.33	0.99	0.72		I
And CK	23106+4214	2449589.145	6.61	5.80	5.62	5.66		I
And DV	23021+3806	2449589.162	6.18	5.50	5.30	5.28		I
And EI	01045+4520	2449587.053	3.53	2.66	2.35	2.11		I
And ES	23093+4843	2449589.129	2.78	1.84	1.48	1.18		I
And FG	00414+4447	2449587.134	5.23	4.28	3.97	3.87		I
And GL	23524+4506	2449587.117	5.34	4.49	4.28	4.23		I
And UY	02352+3857	2449595.212	5.84	4.88	4.44	4.03		I
Ant AE	10097−3220	2449383.335	3.44	2.56	2.16	1.77	1.89	M
Ant RR		2449383.191	2.16	1.21	0.88	0.58	1.02	M
Ant TU		2449383.199	7.60	6.85	6.60	6.59	7.56	M
Ant U	10329−3918		1.10	−0.02	−0.60	−1.18	−0.65	K
Ant U	10329−3918	2449383.350	1.17	0.08	−0.51	−1.12	−0.52	M
Aps U	15219−7545		3.60	2.41	1.81	1.11	1.57	K
Aps V	14598−7124		2.82	1.80	1.40	1.07	1.29	K
Aps W	17079−7405		2.59	1.65	1.26	0.90	1.21	K
Aql TZ	20276−0455		2.45	1.46	1.13	0.80	1.00	K
Aql V1261	19323+0702	2449856.231	4.02	3.11	2.85	2.64		I
Aql V1263	19326+0158		3.86	2.85	2.45	2.15	2.45	K
Aql V373	19267+0642		4.98	3.90	3.44	3.00	3.20	K
Aql V463	19450+1338		4.64	3.61	3.24	2.91	3.21	K
Aql V490	18561+1255		4.33	3.27	2.82	2.49	2.74	K
Aql V584	20079−0146		2.15	1.19	0.77	0.42	0.58	K
Aql V842	19113+0232	2449856.214	2.48	1.56	1.23	0.96		I
Aqr AB	22359−1417		2.45	1.44	1.05	0.71	0.92	K
Aqr SV	23201−1105		2.43	1.46	1.05	0.70	0.98	K
Ari RY	01597+1601	2449590.182	2.87	1.98	1.66	1.44		I
Ari SW	02022+1910	2449590.192	5.43	4.51	4.25	4.08		I
Ari TW	02270+1549	2449590.203	3.99	3.06	2.75	2.60		I
Aur FI	04588+4205	2449670.069	5.15	4.20	3.85	3.68		I
Boo BV		2449855.996	9.30	8.60	8.46			I
Boo CF	14064+4941	2449853.991	1.98	1.15	0.95	0.70		I
Boo CH	14329+4935	2449852.028	2.81	2.05	1.88	1.76		I
Boo CI	14200+2935	2449850.990	1.74	0.86	0.60	0.36		I
Boo XZ	13515+1731	2449850.977	3.89	3.01	2.74	2.51		I
Car RU	09143−6601	2449383.237	5.53	4.46	3.98	3.48	3.87	M
Car SY	11134−5739	2449383.320	4.84	3.87	3.46	3.06	3.54	M
Car UV	10226−6039		4.30	3.20	2.76	2.31	2.08	K
Car UV	10226−6039	2449383.281	4.19	3.14	2.73	2.31	2.29	M
Cas AA	01163+5604	2449594.167	2.65	1.76	1.46	1.30		I
Cas EH	23431+6204	2449596.093	4.42	3.37	2.97	2.71		I
Cas NQ	00218+5400	2449596.129	5.30	4.45	4.05	3.52		I
Cas OO	00411+5839	2449591.160	4.79	3.80	3.43	3.22		I
Cas V356	23268+5622	2449590.130	3.66	2.65	2.25	1.94		I
Cas V398	23202+5901	2449590.119	3.11	2.07	1.59	0.98		I
Cas V416	00589+5659	2449591.180	6.39	5.47	5.16	4.76		I

⟶

Table 3. continued

GCVS4	IRAS	JD	J	H	K	L'	M	c
Cas V446	00333+6224	2449596.146	3.48	2.55	2.28	2.19		I
Cas V451	00493+5927	2449595.130	3.00	2.09	1.80	1.63		I
Cas WW	01302+5729	2449587.185	4.35	3.10	2.38	1.71		I
Cas XZ	01196+6054	2449594.178	5.40	4.54	4.28	4.26		I
Cas XZ	01196+6054	2449595.163	5.36	4.52	4.26	4.13		I
Cen V434	11096−3553	2449382.333	4.58	3.64	3.34	3.10	3.51	M
Cet SW	01359+0106	2449595.182	3.39	2.51	2.20	2.02		I
CMa BE	07215−2252		4.66	3.62	3.12	2.49	2.84	K
CMa DT	07153−1407		5.82	4.79	4.38	4.05	4.64	K
CMa W	07057−1150		2.59	1.52	1.01	0.48	0.85	K
Cnc BL	08033+2246	2449851.884	2.34	1.52	1.30	1.10		I
Cnc UV	08358+2120	2449670.252	3.97	3.05	2.88	2.63		I
Com TW	12161+2222	2449852.977	4.89	4.03	3.78	3.56		I
CrB SX	16134+3327	2449851.084	4.16	3.31	3.06	2.89		I
Crv S	12349−1659	2449382.357	3.65	2.72	2.37	2.08	2.42	M
CVn VY	13285+3801	2449855.985	5.19	4.31	4.07	3.79		I
CVn ZZ	13571+4542	2449856.041	3.82	2.94	2.64	2.38		I
Cyg AD	20296+3223	2449590.015	3.36	2.37	2.04	1.76		I
Cyg QZ	19572+3807	2449588.994	6.27	5.38	5.15	5.02		I
Cyg TZ	19147+5004	2449588.954	3.73	2.85	2.53	2.20		I
Cyg V1058	21002+3434	2449595.988	3.34	2.48	2.23	2.13		I
Cyg V1125	19298+3145	2449856.222	4.11	3.21	2.95	2.74		I
Cyg V1172	19562+3304	2449588.979	4.14	3.21	2.89	2.60		I
Cyg V1335	21194+4537	2449589.097	5.82	4.95	4.69	4.41		I
Cyg V1351	19409+5520	2449854.170	1.57	0.68	0.42	0.21		I
Cyg V397	20302+3517	2449590.028	3.17	2.22	1.79	1.38		I
Cyg V417	19592+3933	2449589.010	6.61	5.66	5.30	4.92		I
Cyg V582	21101+4622	2449589.030	5.56	4.55	4.22	4.05		I
Cyg V590	21155+4529	2449589.062	3.68	2.71	2.36	2.11		I
Cyg V591	21156+4558	2449589.078	5.71	4.76	4.47	4.29		I
Cyg V594	21184+4305	2449671.897	5.42	4.38	3.98	3.74		I
Cyg V890	19315+3203	2449589.972	5.73	4.82	4.56	4.45		I
Cyg V895	19318+3236	2449589.986	6.48	5.58	5.35	4.76		I
Cyg V918	19357+3006	2449586.973	4.57	3.61	3.30	3.05		I
Del CT	20270+0943	2449594.964	2.16	1.31	1.02	0.84		I
Dra AT	16164+5952	2449853.058	1.12	0.29	0.04	−0.16		I
Dra BB	17528+5703	2449588.898	3.22	2.37	2.04	1.73		I
Dra TY	17361+5746	2449854.157	2.28	1.36	0.99	0.69		I
Dra UW	17565+5440	2449588.911	4.68	4.00	3.86	3.81		I
Gem AB	06232+1906		4.60	3.37	2.60	1.79	2.32	K
Gem AP	06234+1600		6.57	5.49	5.11	4.78	5.02	K
Gem BL	06314+1427		4.97	3.94	3.58	3.31	3.53	K
Gem CR	06315+1606		3.36	2.07	1.46	0.88	1.10	K
Her CV	16366+3057	2449589.904	4.98	4.13	3.82	3.38		I
Her GN	16302+3857	2449852.040	4.66	3.78	3.55	3.37		I
Her IY	18496+2520	2449590.971	5.53	4.59	4.31	4.11		I
Her OU	18010+2829	2449589.935	4.90	4.02	3.75	3.58		I
Her V350	17196+2448	2449590.938	5.35	4.45	4.16	3.80		I
Her V449	16412+4829	2449852.066	3.96	3.10	2.86	2.66		I
Her V456	17046+2110	2449590.908	4.62	3.71	3.29	2.83		I

⟶

Table 3. continued

GCVS4	IRAS	JD	J	H	K	L'	M	c
Her V457	17062+2046	2449590.922	4.74	3.86	3.56	3.30		I
Her V479	17192+1836		5.09	4.14	3.64	3.33	3.63	K
Her V508	17364+3142	2449589.920	4.39	3.49	3.19	2.99		I
Her V522	17457+4002	2449586.885	6.16	5.38	5.19	4.27		I
Her V636	16457+4219	2449853.075	1.66	0.84	0.61	0.38		I
Her V640	17236+1657	2449853.093	1.70	0.87	0.62	0.40		I
Hya AR	09236−2332	2449383.184	3.47	2.53	2.20	1.91	2.30	M
Hya BK	11176−3458	2449382.348	4.57	3.65	3.36	3.12	3.55	M
Hya FH	09315−0645	2449855.899	6.04	5.19	4.92	4.85		I
Hya FK	08220−0821	2449855.884	1.54	0.68	0.38	0.14		I
Hya FZ	08189+0507		1.68	0.72	0.35	0.01	0.25	K
Hya GH	13540−2654	2449853.018	4.05	3.16	2.90	2.73		I
Hya HW		2449383.225	4.80	3.92	3.64	3.59	3.83	M
Hya HY	11121−2548	2449382.340	2.77	1.91	1.60	1.37	1.77	M
Hya IZ	10256−2108	2449383.342	3.09	2.16	1.78	1.44	1.62	M
Lac FO	22498+5042	2449590.089	4.09	3.17	2.77	2.42		I
Lac FW	22193+4523	2449596.036	2.52	1.58	1.26	1.11		I
Lac TV	22539+5357	2449590.104	4.91	3.96	3.52	3.02		I
Leo AI	11378+1128	2449851.935	4.39	3.51	3.24	3.00		I
Leo UY	10266+2319	2449851.906	3.67	2.80	2.52	2.25		I
Leo WX	11536+1600	2449851.946	3.44	2.59	2.33	2.14		I
Lib FZ	15166−0857	2449851.025	2.13	1.26	1.00	0.76		I
LMi RS	09254+3622	2449851.894	2.65	1.76	1.45	1.16		I
Lyr EY	18389+3137	2449595.927	3.73	2.84	2.56	2.37		I
Lyr HK	18410+3654	2449586.931	3.23	2.15	1.62	0.99		I
Lyr HM	18505+3327	2449589.960	2.95	2.03	1.71	1.43		I
Lyr T	18306+3657	2449595.899	2.48	1.28	0.41	−0.49		I
Lyr UY	18522+4637	2449588.942	4.42	3.55	3.21	2.85		I
Lyr V398	19065+3904	2449593.957	1.91	1.03	0.72	0.52		I
Lyr X	19110+2641	2449595.940	4.99	4.08	3.80	3.67		I
Lyr YZ	19014+2904	2449590.987	3.58	2.64	2.25	1.88		I
Mon AP	07071−0639		4.73	3.79	3.49	3.32	3.67	K
Mon BQ	07020−0953		3.96	2.71	2.20	1.77	2.09	K
Mon BR	07048−0114		5.88	4.91	4.58	4.30	4.59	K
Mon CX	06347+0057		4.33	3.12	2.65	2.27	2.79	K
Mon DL	06492+0514		7.07	5.63	4.78	3.95	4.56	K
Mon EL	06523−0636		5.01	4.00	3.60	3.20	3.39	K
Mon EU	06588−0527		6.70	5.39	4.73	4.06	4.34	K
Mon EX	06595−0801		6.02	4.99	4.58	4.24	4.40	K
Mon W	06499−0705		4.83	3.70	3.11	2.47	2.89	K
Mon WX	06414−0444		7.05	6.06	5.70	5.37	5.42	K
Mus BO	12319−6728	2449383.367	0.43	−0.52	−0.88	−1.11	−0.77	M
Mus μ	11458−6632	2449383.358	2.00	1.26	1.07	0.95	1.26	M
Oph TY	18289+0420		3.79	2.49	1.81	1.05	1.49	K
Oph V551	17377−2722	2449854.107	4.21	3.33	3.08	2.95		I
Oph V649	18356+0920		4.94	3.92	3.52	3.17	3.46	K
Oph V679	18395+0646	2449854.125	4.01	3.05	2.76	2.50		I
Oph V679	18395+0646	2449856.205	3.97	3.00	2.72	2.46		I
Oph V914	17570+1147	2449853.145	4.31	3.44	3.17	3.07		I
Ori DD	06189+1315		3.96	2.79	2.41	2.04	2.29	K

⟶

Table 3. continued

GCVS4	IRAS	JD	J	H	K	L'	M	c
Ori DR	05594+0827		4.04	3.04	2.66	2.28	2.47	K
Ori EN	06149+0858		5.83	4.86	4.49	4.15	4.38	K
Ori EX	05220−0611		2.51	1.53	1.13	0.73	0.81	K
Ori V352	05592−0221		1.13	0.14	−0.22	−0.51	−0.30	K
Ori V520	05413+0656		4.47	3.48	3.10	2.81	3.01	K
Ori V535	05208−0436		3.56	2.63	2.22	1.82	2.04	K
Peg AD	22218+2629	2449590.043	5.42	4.50	4.21	3.93		I
Peg DW	21299+2415	2449671.914	3.74	2.81	2.48	2.30		I
Peg EO	23142+1019	2449595.112	1.59	0.72	0.38	0.22		I
Peg EV	21462+0658		4.70	3.78	3.38	2.91	2.92	K
Peg EW	22443+2504	2449590.058	3.48	2.55	2.19	1.90		I
Peg GI	22043+2443	2449591.048	3.41	2.51	2.17	1.96		I
Peg GM	22280+1250	2449591.062	2.55	1.65	1.26	0.84		I
Peg GO	22525+1917	2449596.073	3.02	2.12	1.86	1.77		I
Peg GQ	23466+2621	2449587.027	5.07	4.11	3.77	3.54		I
Peg UY	22423+3001	2449587.015	5.08	4.13	3.89	3.82		I
Per GQ	04200+3605	2449672.061	3.72	2.71	2.36	2.20		I
Per UU	03433+5231	2449587.235	3.66	2.51	2.06	1.71		I
Pic W	05418−4628		2.97	1.69	1.02	0.14	0.64	K
Psc TW	00371+1355	2449591.118	3.55	2.65	2.30	2.09		I
Psc TX	23438+0312		0.83	−0.25	−0.70	−1.15	−0.87	K
Pup AC	08204−1545	2449855.870	4.23	3.20	2.59			I
Pup FV	07302−1207		4.97	3.96	3.63	3.37	3.58	K
Pup FW	07303−1239		6.00	5.01	4.64	4.34	4.51	K
Pup GG	07360−1556		4.06	3.02	2.61	2.36	2.89	K
Pup IK	08015−2341		6.11	4.80	4.11	3.34	3.89	K
Pup IM	08024−2514		5.47	4.41	4.05	3.75	3.88	K
Pyx UY	09103−2618	2449383.177	3.93	3.02	2.68	2.45	2.82	M
Sco V461	17068−3315		4.61	3.45	3.05	2.83	3.08	K
Ser DR	18448+0523		4.12	2.79	2.08	1.38	1.82	K
Ser FL	15097+1909	2449851.015	1.73	0.84	0.60	0.38		I
Ser FQ	16061+0844	2449851.049	1.60	0.72	0.47	0.24		I
Sex Z	10083+0248	2449854.918	4.89	4.01	3.78	3.45		I
Sge BF	20001+2056	2449591.002	4.80	3.75	3.26	2.78		I
Sgr V1943	20038−2722		0.06	−0.92	−1.34	−1.78	−1.59	K
Tau CP	05425+1529		5.00	3.81	3.39	2.73	3.18	K
Tau DU	05273+2150	2449670.121	6.21	5.27	4.98	4.71		I
Tau DV	05281+1831	2449670.137	2.53	1.64	1.35	1.15		I
Tau DY	05390+1831	2449672.125	3.82	2.86	2.55	2.36		I
Tau SY	03457+2322	2449672.019	4.86	3.95	3.67	3.52		I
Tau WZ	03441+2014	2449590.232	4.99	4.06	3.74	3.56		I
Tel Y	20165−5051		1.77	0.81	0.42	0.05	0.24	K
TrA V	16449−6741		4.25	3.22	2.77	2.30	2.59	K
TrA X	15094−6953		1.22	0.01	−0.60	−1.23	−0.75	K
UMa AZ	11445+4344	2449852.951	2.47	1.62	1.30	1.03		I
UMa CG	09180+5654	2449854.890	1.52	0.64	0.40	0.15		I
UMa CO	11065+3634	2449853.927	1.50	0.67	0.43	0.19		I
UMa CV	11047+4926	2449853.913	3.45	2.59	2.30	2.03		I
UMa RT	09149+5136	2449854.901	4.93	3.86	3.25	2.56		I
UMa TT	09013+6029	2449853.870	2.80	1.96	1.68	1.42		I

⟶

Table 3. continued

GCVS4		IRAS	JD	J	H	K	L'	M	c
UMa	WY	10388+5153	2449853.884	4.68	3.78	3.48	3.18		I
Vel	CE	09469−4135	2449383.208	3.83	2.89	2.55	2.29	3.02	M
Vel	EE	09535−4938	2449383.254	5.23	4.11	3.51	2.88	3.46	M
Vel	GY	10147−5057	2449383.262	1.62	0.73	0.42	0.25	0.58	M
Vel	HI	10420+5249	2449383.300	3.34	2.43	2.09	1.88	2.27	M
Vel	HP	10389−5149	2449383.294	3.17	2.24	1.89	1.66	2.00	M
Vel	HQ	10436−5321	2449383.307	3.54	2.69	2.35	2.06	2.42	M
Vel	SS	10507−5309	2449383.313	4.96	3.84	3.26	2.59	3.04	M
Vir	CH	12177−0843	2449853.003	3.02	2.17	1.84	1.55		I
Vir	CL	13406−0951	2449856.008	5.23	4.35	4.06	3.80		I
Vir	ES	14059−0837	2449851.978	3.60	2.72	2.48	2.29		I
Vir	ω	11358+0824	2449851.925	0.88	0.01	−0.23	−0.45		I
Vir	ψ	12517−0915	2449851.968	1.22	0.36	0.15	−0.04		I
Vir	RW	12046−0629		1.49	0.56	0.21	−0.11	0.20	K
Vul	CO	19415+1926		5.70	4.12	3.15	2.14	2.35	K
Vul	DY	21012+2347	2449596.023	1.03	0.12	−0.17	−0.26		I
Vul	FI	20466+2248	2449595.975	1.30	0.41	0.12	−0.01		I
Vul	HH	19501+2906	2449586.986	4.58	3.61	3.30	3.14		I
Vul	IN	20511+2523	2449591.035	2.67	1.75	1.37	0.98		I
Vul	IX	19368+2618	2449586.971	6.07	5.10	4.84	4.88		I